

# Spontaneous $\mathcal{PT}$ -symmetry breaking in complex frequency band structures

Vassilios Yannopoulos\*

*Department of Physics, National Technical University of Athens, GR-15780 Athens, Greece*

(Received 18 November 2013; published 10 January 2014)

We demonstrate that the process of band-gap creation in periodic solids such as atomic, photonic, or phononic crystals can be viewed as spontaneous  $\mathcal{PT}$ -symmetry breaking in the framework of a complex frequency band structure. This allows the use of ordinary artificial structures such as Bragg stacks and simple photonic crystals as suitable test beds for the study of phenomena related to  $\mathcal{PT}$ -symmetry breaking.

DOI: [10.1103/PhysRevA.89.013808](https://doi.org/10.1103/PhysRevA.89.013808)

PACS number(s): 42.70.Qs, 42.25.Bs, 78.67.Pt, 11.30.Er

## I. INTRODUCTION

Systems with combined parity ( $\mathcal{P}$ ) and time ( $\mathcal{T}$ ) symmetry, i.e., possessing  $\mathcal{PT}$  symmetry, have attracted significant interest recently in various areas such as quantum field theory [1,2], open quantum systems [3,4], and photonics [5–9]. In quantum theory,  $\mathcal{PT}$ -symmetric systems are those possessing a non-Hermitian Hamiltonian which, however, respects parity-time ( $\mathcal{PT}$ ) requirements. Given that the action of the parity operator  $\hat{P}$  is  $\hat{p} \rightarrow -\hat{p}$ ,  $\hat{x} \rightarrow -\hat{x}$  and of the time operator  $\hat{T}$  is  $\hat{p} \rightarrow -\hat{p}$ ,  $\hat{x} \rightarrow \hat{x}$ ,  $i \rightarrow -i$ , it turns out that non-Hermitian Hamiltonian operators  $\hat{H} = \hat{p}^2/2 + V(\hat{x})$  ( $\hbar = m = 1$ ) obeying the symmetry  $V(x) = V^*(-x)$  may possess a real eigenvalue spectrum [1]. This is, however, a necessary but not sufficient condition for the existence of a purely real eigenvalue spectrum. Indeed, in  $\mathcal{PT}$  systems the eigenvalue spectrum becomes generally complex above a certain parameter value signifying a spontaneous  $\mathcal{PT}$ -symmetry breaking, i.e., a phase transition from the exact to broken- $\mathcal{PT}$  phase [10–12]. Namely, a spontaneous  $\mathcal{PT}$ -symmetric breaking usually manifests itself by the occurrence of an exceptional point where two real eigenvalues together with their eigenvectors coalesce into a single, generally complex, eigenvalue. Exceptional points in the parameter space of a non-Hermitian operator are associated with topological charge and geometric (Berry) phase [13].

In the field of optics, the formal equivalence of the Schrödinger equation with the Helmholtz equation in the paraxial (weakly guiding) approximation has led to the introduction of systems with  $\mathcal{PT}$ -symmetric refractive index profiles,  $n(x) = n^*(-x)$  as an experimental testing ground for spontaneous  $\mathcal{PT}$ -symmetry breaking [12,14,15]. Since the refractive index is a general complex quantity,  $n = n_R + in_I$ ,  $\mathcal{PT}$  symmetry is realized via the symmetries  $n_R = n_R(-x)$  and  $n_I(x) = -n_I(-x)$ . Although the first requirement for the real part  $n_R$  is trivially satisfied, the second one needs an experimental setup with materials containing the same amount of gain ( $n_I < 0$ ) and loss ( $n_I > 0$ ). The emergence of  $\mathcal{PT}$ -phase transitions in systems with gain-loss profiles is accompanied with fruitful phenomena such as double refraction [6], power oscillations [6,12,16], coherent perfect absorption, and lasing [16–21]. Analogous phenomena have also been observed in antisymmetric  $\mathcal{PT}$  systems realized by

alternating materials of opposite values of the real part of the refractive index [22].

The need for complex optical potentials which, in turn, requires the inclusion of materials with gain exactly compensating the loss in another (complementary) material constitutes a challenging experimental setup since it involves continuous external pumping of the gain material. The introduction of a compensated gain-loss refractive index profile is needed when one works with the equivalence of the paraxial Helmholtz equation with the Schrödinger one which implies that systems with real refractive indexes possess a real eigenvalue spectrum. However, in optics, there are various examples with systems with a purely complex spectrum, e.g., scattering electromagnetic modes; there, all solutions of the light-scattering problem off a material object possess a complex frequency spectrum due to the finite lifetime of the scattering states. The actual challenge which justifies the need for the use of gain-loss index profile systems is the observation of the  $\mathcal{PT}$ -phase transition from a purely real to a fully or partially complex eigenvalue spectrum.

In this work we show that under the framework of a complex frequency band structure in periodic solids, one can observe the  $\mathcal{PT}$ -phase transition in the formation of frequency band gaps. In particular, we show that the emergence of photonic band gaps in ordinary passive photonic crystals is manifested as a spontaneous  $\mathcal{PT}$ -symmetry breaking which can be easily measured in the laboratory with wave transmission experiments from photonic-crystal slabs of different thicknesses. In the following, after providing a brief overview of the theory of complex band structure we show examples of spontaneous  $\mathcal{PT}$ -symmetry breaking in a one-dimensional (1D) photonic crystal as well as in a magneto-dielectric photonic crystal.

## II. COMPLEX FREQUENCY BAND STRUCTURE

In traditional energy band structure calculations of an electron in an ordinary crystal, or of the frequency band structure of the electromagnetic (EM) field in the case of photonic crystals, one starts with a fixed value of the reduced wave vector  $\mathbf{k}$ , and by some method or other (in photonic crystals this is usually the plane-wave method) one solves the eigenvalue problem, for the given  $\mathbf{k}$ , to obtain all the eigenfrequencies within a very wide frequency range, and the corresponding eigenmodes of the scalar or vector field under consideration. These eigenmodes are, in an infinite crystal,

\*vyannop@mail.ntua.gr

propagating Bloch waves which have the property

$$\begin{aligned} \psi_{\mathbf{k}\alpha}(\mathbf{r} + \mathbf{R}_n^{(3)}) \exp[-i\omega_\alpha(\mathbf{k})t] \\ = \exp(i\mathbf{k} \cdot \mathbf{R}_n^{(3)}) \psi_{\mathbf{k}\alpha}(\mathbf{r}) \exp[-i\omega_\alpha(\mathbf{k})t], \end{aligned} \quad (1)$$

where  $\mathbf{R}_n^{(3)}$  is any vector of the three-dimensional (3D) lattice which defines the periodicity of the infinite crystal; and  $\alpha$  is a band index which defines the different frequency bands  $\omega_\alpha(\mathbf{k})$  and the corresponding eigenmodes. For the Schrödinger field (electrons in a crystal)  $\psi$  is a scalar quantity; in the case of the EM field  $\psi$  is a vector quantity. Irrespective of the type of the wave field, the above eigenproblems provide a *real* eigenenergy spectrum by definition.

On-shell methods [23–32] proceed differently; the frequency is fixed and one obtains the eigenmodes of the crystal for this frequency. One views the crystal as a succession of layers parallel to a given crystallographic plane of the crystal. The layers have the same two-dimensional (2D) periodicity (that of the chosen crystallographic plane) described by a 2D lattice:

$$\mathbf{R}_n = n_1 \mathbf{a}_1 + n_2 \mathbf{a}_2, \quad (2)$$

where  $\mathbf{a}_1$  and  $\mathbf{a}_2$  are primitive vectors of the said plane (which is taken to be the  $xy$  plane), and  $n_1, n_2 = 0, \pm 1, \pm 2, \dots$ . We may number the sequence of layers which constitute the infinite crystal, extending from  $z = -\infty$  to  $z = +\infty$ , as follows:  $\dots - 2, -1, 0, 1, 2, \dots$ . The  $(N+1)$ th layer is obtained from the  $N$ th layer by a primitive translation to be denoted by  $\mathbf{a}_3$ . Obviously,  $\mathbf{a}_1, \mathbf{a}_2$ , and  $\mathbf{a}_3$  constitute a basis for the 3D space lattice of the infinite crystal.

We define the 2D reciprocal lattice corresponding to Eq. (2):

$$\mathbf{g} = m_1 \mathbf{b}_1 + m_2 \mathbf{b}_2, \quad m_1, m_2 = 0, \pm 1, \pm 2, \dots, \quad (3)$$

where  $\mathbf{b}_i \cdot \mathbf{a}_j = 2\pi \delta_{ij}$ ,  $i, j = 1, 2$ . The reduced  $(k_x, k_y)$  zone associated with the above, which has the full symmetry of the given crystallographic plane is known as the surface Brillouin zone (SBZ) (see, e.g., Ref. [33]). We define a corresponding 3D reduced  $\mathbf{k}$  zone as follows:

$$\mathbf{k}_\parallel \equiv (k_x, k_y) \text{ within the SBZ, } -|\mathbf{b}_3|/2 < k_z \leq |\mathbf{b}_3|/2, \quad (4)$$

where  $\mathbf{b}_3 = 2\pi \mathbf{a}_1 \times \mathbf{a}_2 / [\mathbf{a}_1 \cdot (\mathbf{a}_2 \times \mathbf{a}_3)]$  is normal to the chosen crystallographic plane. The reduced  $\mathbf{k}$  zone defined by Eq. (4) is of course completely equivalent to the commonly used, more symmetrical Brillouin zone (BZ), in the sense that a point in one of them lies also in the other or differs from such a one by a vector of the 3D reciprocal lattice.

Let us now assume that we have a photonic crystal consisting of nonoverlapping spherical scatterers in a host medium of different dielectric function and let us look at the structure as a sequence of layers of spheres with the 2D periodicity of Eq. (2). A Bloch wave solution, of given frequency  $\omega$  and given  $\mathbf{k}_\parallel$ , of Maxwell's equations for the given system has the following form in the space between the  $N$ th and the  $(N+1)$ th layers (we write down only the electric-field component of the EM wave):

$$\begin{aligned} \mathbf{E}(\mathbf{r}) = \sum_{\mathbf{g}} \{ \mathbf{E}_{\mathbf{g}}^+(N) \exp[i\mathbf{K}_{\mathbf{g}}^+ \cdot (\mathbf{r} - \mathbf{A}_N)] + \mathbf{E}_{\mathbf{g}}^-(N) \\ \times \exp[i\mathbf{K}_{\mathbf{g}}^- \cdot (\mathbf{r} - \mathbf{A}_N)] \}, \end{aligned} \quad (5)$$

with

$$\mathbf{K}_{\mathbf{g}}^\pm = (\mathbf{k}_\parallel + \mathbf{g}, \pm [q^2 - (\mathbf{k}_\parallel + \mathbf{g})^2]^{1/2}), \quad (6)$$

where  $q$  is the wave number, and  $\mathbf{A}_N$  is an appropriate origin of coordinates in the host region between the  $N$ th and the  $(N+1)$ th layers. A similar expression (with  $N$  replaced by  $N+1$ ) gives the electric field between the  $(N+1)$ th and the  $(N+2)$ th layers. Naturally the coefficients  $\mathbf{E}_{\mathbf{g}}^\pm(N+1)$  are related to the  $\mathbf{E}_{\mathbf{g}}^\pm(N)$  coefficients through the scattering matrices of the  $N$ th layer of spheres. We have

$$\begin{aligned} E_{\mathbf{g}i}^-(N) &= \sum_{\mathbf{g}'i'} Q_{\mathbf{g}i;\mathbf{g}'i'}^{\text{IV}} E_{\mathbf{g}'i'}^-(N+1) + \sum_{\mathbf{g}'i'} Q_{\mathbf{g}i;\mathbf{g}'i'}^{\text{III}} E_{\mathbf{g}'i'}^+(N), \\ E_{\mathbf{g}i}^+(N+1) &= \sum_{\mathbf{g}'i'} Q_{\mathbf{g}i;\mathbf{g}'i'}^{\text{I}} E_{\mathbf{g}'i'}^+(N) + \sum_{\mathbf{g}'i'} Q_{\mathbf{g}i;\mathbf{g}'i'}^{\text{II}} E_{\mathbf{g}'i'}^-(N+1), \end{aligned} \quad (7)$$

where  $i = x, y, z$ , and  $\mathbf{Q}$  are appropriately constructed transmission or reflection matrices for the layer (see Fig. 1). For a detailed description of these matrices, which are functions of  $\omega, \mathbf{k}_\parallel$ , the scattering properties of the individual scatterer (sphere), and the geometry of the layer, see Refs. [25,26].

A generalized Bloch wave, by definition, has the property

$$\begin{aligned} \mathbf{E}_{\mathbf{g}}^\pm(N+1) &= \exp(i\mathbf{k} \cdot \mathbf{a}_3) \mathbf{E}_{\mathbf{g}}^\pm(N), \\ \mathbf{k} &= (\mathbf{k}_\parallel, k_z(\omega, \mathbf{k}_\parallel)), \end{aligned} \quad (8)$$

where  $k_z$  may be real or complex. Substituting Eq. (8) into Eq. (7) we obtain

$$\begin{pmatrix} \mathbf{Q}^{\text{I}} & \mathbf{Q}^{\text{II}} \\ -[\mathbf{Q}^{\text{IV}}]^{-1} \mathbf{Q}^{\text{III}} \mathbf{Q}^{\text{I}} & [\mathbf{Q}^{\text{IV}}]^{-1} [\mathbf{I} - \mathbf{Q}^{\text{III}} \mathbf{Q}^{\text{II}}] \end{pmatrix} \begin{pmatrix} \mathbf{E}^+(N) \\ \mathbf{E}^-(N+1) \end{pmatrix} = \exp(i\mathbf{k} \cdot \mathbf{a}_3) \begin{pmatrix} \mathbf{E}^+(N) \\ \mathbf{E}^-(N+1) \end{pmatrix}, \quad (9)$$

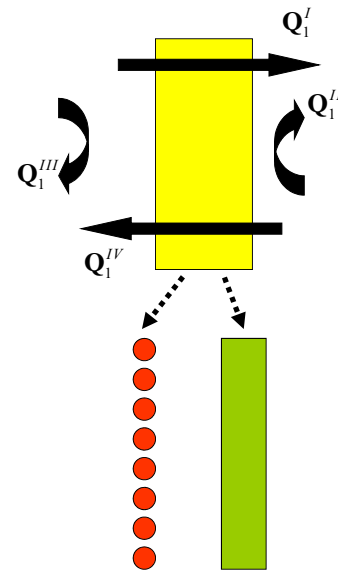


FIG. 1. (Color online) Schematic definition of the scattering  $\mathbf{Q}$  matrices for a finite slab which may be a 2D plane of scatterers or homogeneous slab or any combination of both.

where  $\mathbf{E}^\pm$  are column matrices with the elements  $E_{\mathbf{g}_1x}^\pm, E_{\mathbf{g}_1y}^\pm, E_{\mathbf{g}_1z}^\pm, E_{\mathbf{g}_2x}^\pm, E_{\mathbf{g}_2y}^\pm, E_{\mathbf{g}_2z}^\pm, \dots$ . In practice we keep a finite number of  $\mathbf{g}$  vectors (those with  $|\mathbf{g}| < g_{\max}$ , where  $g_{\max}$  is a cutoff parameter) which leads to a solvable system of equations.

Equation (9) constitutes a typical eigenvalue problem; because the matrix on the left-hand side of Eq. (9) is not Hermitian, its eigenvalues are in general complex numbers. We remember that  $\omega$  and  $\mathbf{k}_\parallel$  are given quantities and therefore the eigenvalues of the matrix on the left-hand side of Eq. (9) determine  $k_z$ ; depending on the number of  $\mathbf{g}$  vectors we keep in the calculation, we obtain a corresponding number of  $k_z$  eigenvalues for the given  $\omega, \mathbf{k}_\parallel$ . These eigenvalues of  $k_z$  looked upon as functions  $k_z = k_z(\omega; \mathbf{k}_\parallel)$  of real  $\omega$ , for given  $\mathbf{k}_\parallel$ , are known as the frequency lines in the complex  $k_z$  space. We refer to them as the complex band structure of the crystal associated with the crystallographic surface defined by Eq. (2). A line  $k_z(\omega; \mathbf{k}_\parallel)$  may be real (in the sense that  $k_z$  is real) over certain frequency regions, and be complex (in the sense that  $k_z$  is complex) for  $\omega$  outside these regions. When  $k_z$  is real, the corresponding Bloch waves, eigensolutions of Eq. (9), represent propagating modes of the EM field in the given crystal. When  $k_z$  is complex, the corresponding Bloch wave is an evanescent wave; it has an amplitude which increases exponentially in the positive or negative  $z$  direction and, unlike the propagating waves, a Bloch wave of this nature does not exist as a physical entity in the infinite crystal. Such states, however, are very useful in understanding the optical properties of finite slabs of the crystal. For example, the attenuation of a wave of given  $\mathbf{k}_\parallel$ , incident on a slab of the material of thickness  $d$ , with a frequency within a region over which no propagating solution exists for the given  $\mathbf{k}_\parallel$ , is determined by that evanescent wave, which has the  $k_z$  with the smallest in magnitude imaginary part  $q_I$ ; the attenuation is roughly speaking proportional to  $\exp(-q_I d)$ . In all cases  $[\mathbf{k}_\parallel, \text{Re}(k_z)]$  lies in the reduced zone defined by Eq. (4).

### III. $\mathcal{PT}$ -SYMMETRY BREAKING IN PASSIVE PHOTONIC CRYSTALS

As a first example of a system exhibiting certain regions of spontaneous  $\mathcal{PT}$ -symmetry breaking is a 1D photonic crystal made of alternating dielectric and air slabs. Namely, the unit cell of the 1D photonic crystal consists of an indium tin oxide (ITO) slab ( $\epsilon = 3.8$ ) of (scaled) thickness  $t\omega/c = 2.0$  which is separated from the next ITO slab of the subsequent unit cell by the distance  $h\omega/c = 1.0$ . These two lengths provide one period of  $d\omega/c = (t + h)\omega/c = 3$  (all lengths are displayed in  $c/\omega$  units,  $\omega$  being the angular frequency, due to the scaling property of Maxwell's equations when materials with constant electric permittivity and/or permeability are used).

Figure 2(a) shows the complex frequency band structure for  $\mathbf{k}_\parallel = \mathbf{0}$  for the above 1D photonic crystal. Figure 2(b) shows the transmittance of light also for normal incidence ( $\mathbf{k}_\parallel = \mathbf{0}$ ) on a finite slab of the 1D photonic crystal consisting of eight unit layers (cells). The spectral regions of suppressed transmittance correspond to band-gap regions. In the complex frequency band structure of Fig. 2(a), the band gaps are manifested as regions of complex  $k_z = \text{Re } k_z + i \text{Im } k_z$  where  $\text{Re } k_z$  assumes the constant values 0 or  $\pi/d$  within the gap regions. The edges of a region with  $\text{Re } k_z = 0$  correspond to exceptional points

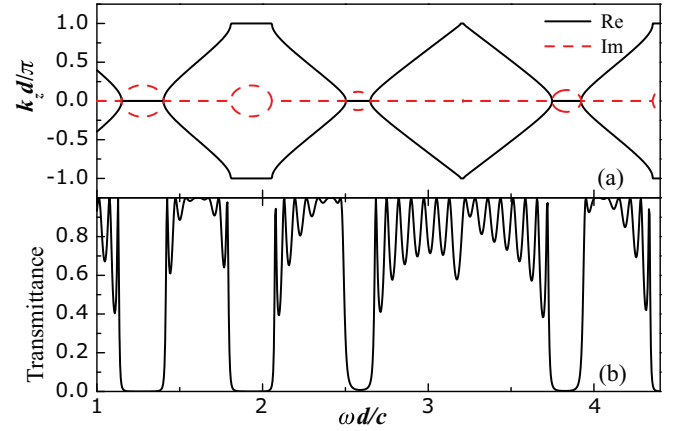


FIG. 2. (Color online) (a) Complex frequency band structure in dimensionless units for a 1D photonic crystal (Bragg stack) made of alternating ITO layer ( $\epsilon = 3.8$ ) of thickness  $t\omega/c = 2.0$  and interlayer distance  $h\omega/c = 1.0$  [period  $d\omega/c = (t + h)\omega/c = 3$ ]. (b) Transmittance of light incident normally ( $\mathbf{k}_\parallel = \mathbf{0}$ ) on finite slab of the above 1D photonic crystal consisting of eight unit layers.

in the frequency band diagram. On the other hand,  $\text{Im } k_z$  exhibits a dispersion with frequency. As pointed out in the previous section, Bloch waves with nonzero  $\text{Im } k_z$  correspond to exponentially decaying or amplifying waves within an infinite crystal and, as such, they are not actual solutions of an infinitely periodic crystal. However,  $\text{Im } k_z$  defines the rate of light decay within the gap region and can thus be determined by measuring the transmittance at each frequency as a function of the photonic-crystal slab thickness. Away from the gap regions,  $k_z$  is purely real corresponding to propagating Bloch waves. Obviously, the band-gap edges are viewed as the onset of the spontaneous  $\mathcal{PT}$ -symmetry breaking which separates the purely real  $k_z$  eigenvalues from the complex ones. If the  $\mathcal{PT}$  phase transition is to be probed experimentally, the real eigenvalues of  $k_z$  are measured by standard interferometry as

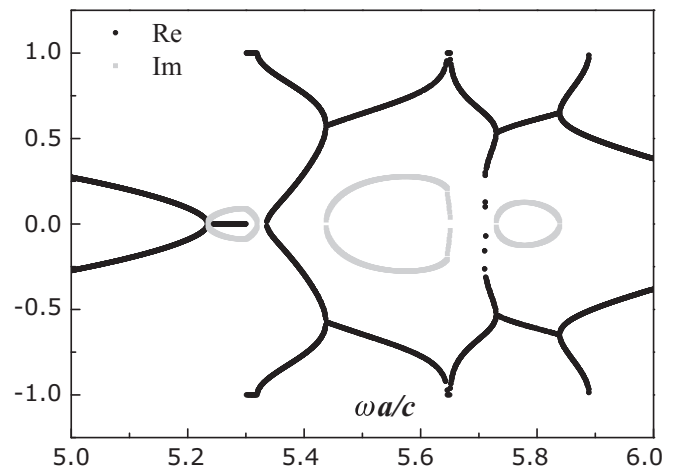


FIG. 3. Complex frequency band structure in dimensionless units for a simple cubic lattice of magnetodielectric spheres ( $\epsilon = 3, \mu = 3$ ) in air ( $\epsilon = 1$ ) with radius  $S\omega/c = 0.2$  and lattice constant  $a\omega/c = 1$ . The complex frequency bands are calculated for  $\mathbf{k}_\parallel = (0.25, 0)\pi/a$ .

they correspond to propagating waves. As stated above,  $\text{Im } k_z$  is determined by light-attenuation experiments.

In the example of the 1D photonic crystal of Fig. 2, the  $\text{Re } k_z$  within the  $\mathcal{PT}$ -symmetry-breaking regions (band gaps) shows no dispersion (constant with frequency). This is not always the case, however. In Fig. 3 we show the complex frequency band structure of a simple cubic crystal consisting of magnetodielectric spheres ( $\epsilon = \mu = 3$ ) of radius  $S\omega/c = 0.2$  and lattice constant  $a\omega/c = 1$ . The band structure is calculated for  $\mathbf{k}_{\parallel} = (0.25, 0)\pi/a$ . One can easily identify several bifurcation (exceptional) points as well as  $\mathcal{PT}$ -symmetry-breaking regions where both  $\text{Re } k_z$  and  $\text{Im } k_z$  are dispersive. Note in passing, that by choosing  $\epsilon = \mu$  for the spheres of the photonic crystal, we have imposed a double degeneracy in the photonic band structure for all  $\mathbf{k}_{\parallel}$  within the SBZ. Had we chosen  $\epsilon \neq \mu$ , the complex frequency bands of Fig. 3 would have split into two non-degenerate bands, in which case the exceptional point would involve the coalescence of four distinct bands into two bands.

#### IV. CONCLUSION

Based on the theory of complex frequency band structure we have demonstrated that the emergence of frequency band gaps in ordinary photonic crystals is translated to regions of spontaneously broken parity-time ( $\mathcal{PT}$ ) symmetry. The parity-time phase transitions can be traced experimentally by interferometric measurements in regions of purely real spectrum of propagation constants while by wave-attenuation experiments one can study the regions of complex spectrum. The experimental setups needed to measure the spontaneous ( $\mathcal{PT}$ ) symmetry breaking in complex frequency bands are less sophisticated than those required in loss-gain systems. Since the theory of complex frequency band structure is a universal theory and applies to other physical solids such as ordinary atomic crystals as well as phononic crystals [34,35], we expect the phenomenon of  $\mathcal{PT}$ -symmetry breaking to be evident in those systems, too.

- 
- [1] C. M. Bender and S. Boettcher, *Phys. Rev. Lett.* **80**, 5243 (1998); C. M. Bender, D. C. Brody, and H. F. Jones, *ibid.* **89**, 270401 (2002); C. M. Bender, *Am. J. Phys.* **71**, 1095 (2003); C. M. Bender, D. C. Brody, H. F. Jones, and B. K. Meister, *Phys. Rev. Lett.* **98**, 040403 (2007).
- [2] I. Y. Goldsheid and B. A. Khoruzhenko, *Phys. Rev. Lett.* **80**, 2897 (1998); H. Markum, R. Pullirsch, and T. Wettig, *ibid.* **83**, 484 (1999); B. Bagchi and C. Quesne, *Phys. Lett. A* **273**, 285 (2000).
- [3] I. Rotter, *J. Phys. A* **42**, 153001 (2009).
- [4] C. Dembowski, B. Dietz, H.-D. Gräf, H. L. Harney, A. Heine, W. D. Heiss, and A. Richter, *Phys. Rev. Lett.* **90**, 034101 (2003).
- [5] R. El-Ganainy, K. G. Makris, D. N. Christodoulides, and Z. H. Musslimani, *Opt. Lett.* **32**, 2632 (2007).
- [6] K. G. Makris, R. El-Ganainy, D. N. Christodoulides, and Z. H. Musslimani, *Phys. Rev. Lett.* **100**, 103904 (2008).
- [7] T. Kottos, *Nat. Phys.* **6**, 166 (2010).
- [8] A. Regensburger, C. Bersch, M. A. Miri, G. Onishchukov, D. N. Christodoulides, and U. Peschel, *Nature (London)* **488**, 167 (2012).
- [9] L. Feng, Y.-L. Xu, W. S. Fegadolli, M.-H. Lu, J. E. B. Oliveira, V. R. Almeida, Y.-F. Chen, and A. Scherer, *Nat. Mater.* **12**, 108 (2013).
- [10] A. Mostafazadeh, *J. Math. Phys.* **43**, 3944 (2002).
- [11] S. Klaiman, U. Günther, and N. Moiseyev, *Phys. Rev. Lett.* **101**, 080402 (2008).
- [12] C. E. Rüter, K. G. Makris, R. El-Ganainy, D. N. Christodoulides, M. Segev, and D. Kip, *Nat. Phys.* **6**, 192 (2010).
- [13] U. Günther, I. Rotter, and B. F. Samsonov, *J. Phys. A: Math. Theor.* **40**, 8815 (2007); F. Keck, H. J. Korsch, and S. Mossmann, *J. Phys. A: Math. Gen.* **36**, 2125 (2003); A. I. Nesterov and F. Aceves de la Cruz, *J. Phys. A: Math. Theor.* **41**, 485304 (2008).
- [14] L. Feng, M. Ayache, J. Huang, Y.-L. Xu, M.-H. Lu, Y.-F. Chen, Y. Fainman, and A. Scherer, *Science* **333**, 729 (2011).
- [15] J. Schindler, A. Li, M. C. Zheng, F. M. Ellis, and T. Kottos, *Phys. Rev. A* **84**, 040101(R) (2011).
- [16] M. C. Zheng, D. N. Christodoulides, R. Fleischmann, and T. Kottos, *Phys. Rev. A* **82**, 010103(R) (2010).
- [17] Y. D. Chong, L. Ge, H. Cao, and A. D. Stone, *Phys. Rev. Lett.* **105**, 053901 (2010).
- [18] W. Wan, Y. D. Chong, L. Ge, H. Noh, A. D. Stone, and H. Cao, *Science* **331**, 889 (2011).
- [19] S. Longhi, *Phys. Rev. A* **82**, 031801(R) (2010).
- [20] Y. D. Chong, L. Ge, and A. D. Stone, *Phys. Rev. Lett.* **106**, 093902 (2011).
- [21] H. Schomerus, *Phys. Rev. Lett.* **104**, 233601 (2010).
- [22] L. Ge and H. E. Türeci, *Phys. Rev. A* **88**, 053810 (2013).
- [23] K. Ohtaka, *Phys. Rev. B* **19**, 5057 (1979).
- [24] K. Ohtaka and Y. Tanabe, *J. Phys. Soc. Jpn.* **65**, 2265 (1996).
- [25] N. Stefanou, V. Karathanos, and A. Modinos, *J. Phys.: Condens. Matter* **4**, 7389 (1992).
- [26] N. Stefanou, V. Yannopapas, and A. Modinos, *Comput. Phys. Commun.* **113**, 49 (1998); **132**, 189 (2000).
- [27] J. B. Pendry and A. MacKinnon, *Phys. Rev. Lett.* **69**, 2772 (1992).
- [28] P. M. Bell, J. B. Pendry, L. Martín-Moreno, and A. J. Ward, *Comput. Phys. Commun.* **85**, 306 (1995).
- [29] Y. Qiu, K. M. Leung, L. Cavin, and D. Kralj, *J. Appl. Phys.* **77**, 3631 (1995).
- [30] R. C. McPhedran, L. C. Botten, A. A. Asatryan, N. A. Nicorovici, P. A. Robinson, and C. M. de Sterke, *Aust. J. Phys.* **52**, 791 (1999).
- [31] G. Gantzounis, N. Stefanou, and N. Papanikolaou, *Phys. Rev. B* **77**, 035101 (2008).
- [32] V. Yannopapas and A. G. Vanakaras, *Phys. Rev. B* **84**, 085119 (2011).
- [33] A. Modinos, *Field, Thermionic, and Secondary Electron Emission Spectroscopy* (Plenum, New York, 1984).
- [34] I. E. Psarobas, A. Modinos, R. Sainidou, and N. Stefanou, *Phys. Rev. B* **65**, 064307 (2002).
- [35] R. Sainidou, N. Stefanou, and A. Modinos, *Phys. Rev. B* **66**, 212301 (2002).